

## Evidence for Half-Metallicity in $n$ -type $\text{HgCr}_2\text{Se}_4$

Tong Guan, Chaojing Lin, Chongli Yang, Youguo Shi,<sup>\*</sup> Cong Ren,<sup>†</sup> and Yongqing Li<sup>‡</sup>  
*Beijing National Laboratory for Condensed Matter Physics, Institute of Physics,  
 Chinese Academy of Sciences, Beijing 100190, China*

Hongming Weng, Xi Dai, and Zhong Fang  
*Beijing National Laboratory for Condensed Matter Physics, Institute of Physics,  
 Chinese Academy of Sciences, Beijing 100190, China  
 and Collaborative Innovation Center of Quantum Matter, Beijing 100084, China*

Shishen Yan  
*School of Physics, Shandong University, Jinan 250100, China*

Peng Xiong  
*Department of Physics, Florida State University, Tallahassee, Florida 32306, USA*  
 (Received 28 January 2015; revised manuscript received 22 June 2015; published 21 August 2015)

High quality  $\text{HgCr}_2\text{Se}_4$  single crystals have been investigated by magnetization, electron transport, and Andreev reflection spectroscopy. In the ferromagnetic ground state, the saturation magnetic moment of each unit cell corresponds to an integer number of electron spins ( $3 \mu_B/\text{Cr}^{3+}$ ), and the Hall effect measurements suggest  $n$ -type charge carriers. Spin polarizations as high as 97% were obtained from fits of the differential conductance spectra of  $\text{HgCr}_2\text{Se}_4/\text{Pb}$  junctions with the modified Blonder-Tinkham-Klapwijk theory. The temperature and bias-voltage dependencies of the subgap conductance are consistent with recent theoretical calculations based on spin active scatterings at a superconductor-half-metal interface. Our results suggest that  $n$ - $\text{HgCr}_2\text{Se}_4$  is a half-metal, in agreement with theoretical calculations that also predict undoped  $\text{HgCr}_2\text{Se}_4$  is a magnetic Weyl semimetal.

DOI: 10.1103/PhysRevLett.115.087002

PACS numbers: 74.78.Fk, 74.20.Rp, 74.25.Ha, 74.70.Dd

Chromium chalcogenides of the spinel group  $\text{ACr}_2\text{X}_4$  ( $A = \text{Hg}, \text{Cd}, \text{Zn}, X = \text{Se}, \text{S}$ ) have been studied as magnetic semiconductors or insulators for several decades [1–3]. They have attracted much recent interest because the ferromagnetism and band structures are conducive to the emergence of Chern semimetallicity [4]. Chern semimetals (i.e., magnetic Weyl metals) are a class of ferromagnetic materials in which band crossings are guaranteed to exist at certain points in the momentum space by topological protection [4]. In addition to the fascinating Weyl fermion physics [5–7] that was recently observed in their non-magnetic counterparts [8–12], Chern semimetals can also host other interesting phenomena requiring broken time-reversal symmetry, such as the quantized anomalous Hall effect [13,14]. As a candidate proposed for Chern semimetals,  $\text{HgCr}_2\text{Se}_4$  can also be a unique spintronic material due to its  $s$ -band half-metallicity when doped to  $n$ -type [4].

Ferromagnetic order in  $\text{ACr}_2\text{X}_4$  arises at low temperatures due to the superexchange interactions between the 3d electrons of Cr. The  $s$ - $d$  exchange interactions can produce a large spin splitting of the conduction bands [Fig. 1(a)]. Depending on the magnitude of exchange splitting and the strength of spin-orbit coupling, these chalcospinels can be either magnetic semiconductors (e.g.,  $\text{CdCr}_2\text{Se}_4$  [15]) or

Chern semimetals (e.g.,  $\text{HgCr}_2\text{Se}_4$  [4]). Regardless of whether the exchange splitting is strong enough for a band inversion, a common feature of these chromium chalcospinels is that there exists a sizable range of chemical potential for fully spin polarized  $s$ -band conductivity [4,16]; this makes them a unique type of half-metals. Half-metals are a class of magnetic materials in which the charge current is conducted by carriers of one spin orientation [17,18]. In a half-metal, the Fermi level is located either inside an energy gap or in the localized states for one spin direction [19], whereas the electronic states are extended for the other. The complete spin polarization of itinerant carriers makes half-metals very attractive for spintronic applications, such as in high performance magnetic tunnel junctions [20] and for efficient spin injection into semiconductors [21]. Recent theories also suggest that half-metals, especially those with single bands and strong spin-orbit interactions, may host  $p$ -wave or topological superconductivity [22,23] when they are in proximity to  $s$ -wave superconductors [24,25]. So far, however, only a handful of materials have been shown experimentally to be half-metallic [26–29]. Moreover, charge carriers in these materials either have  $d$ -band characteristics [e.g.,  $\text{CrO}_2$  [30],  $(\text{La}, \text{Sr})\text{MnO}_3$  [20,31],  $\text{EuO}$  [32]] or are holes in  $p$  orbitals (e.g.,  $\text{GaMnAs}$ ) [33]. Definitive experimental demonstration

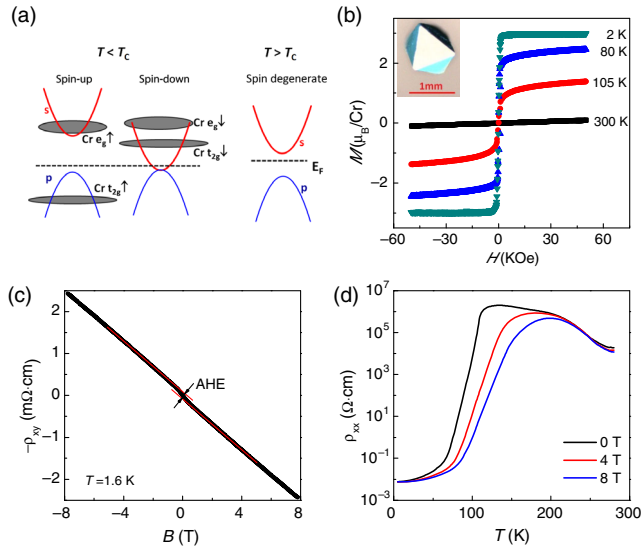


FIG. 1 (color online). (a) Schematic band diagrams for HgCr<sub>2</sub>Se<sub>4</sub> in the ferromagnetic (left) and paramagnetic (right) states based on the first principles calculations reported in Refs. [4,16]. (b) Magnetization curves at several temperatures from  $T = 2$  to 300 K. The inset shows an optical micrograph for a typical HgCr<sub>2</sub>Se<sub>4</sub> crystal. (c) Hall resistivity  $\rho_{xy}$  curve taken at  $T = 1.6$  K. The small curvature near the zero field is due to the anomalous Hall effect (AHE). (d) Temperature dependence of longitudinal resistivity  $\rho_{xx}$  at magnetic fields  $\mu_0 H = 0, 4, 8$  T.

of *s*-band half-metals remains elusive, and no direct measurement of the electron spin polarization has been reported in this spinel class of materials.

In this Letter, we report that measurements of magnetization, electron transport, and Andreev reflection spectra have been carried out on high quality *n*-type HgCr<sub>2</sub>Se<sub>4</sub> single crystals. Exchange splitting induced metal-insulator transition is manifested as 8 orders of magnitude change in longitudinal resistivity upon ferromagnetic ordering as well as colossal magnetoresistance near  $T_C$ . In the ferromagnetic state, the saturation magnetization is found to correspond to  $3.0 \mu_B/\text{Cr}^{3+}$ . The zero-bias conductances of Pb/HgCr<sub>2</sub>Se<sub>4</sub> Andreev junctions are nearly completely suppressed. These results coherently point to *n*-type HgCr<sub>2</sub>Se<sub>4</sub> being a half-metal.

Single crystals of HgCr<sub>2</sub>Se<sub>4</sub> were grown with chemical vapor transport [34]. The single crystalline samples usually are octahedral shaped and  $\sim 1$  mm in size [Fig. 1(b) inset]. As shown in Fig. 1(b), HgCr<sub>2</sub>Se<sub>4</sub> is a soft ferromagnet below the Curie temperature ( $T_C = 105.5$  K), and no hysteresis was clearly resolved. The saturation magnetization  $M_s$  corresponds to  $3.00 \pm 0.05 \mu_B$  per Cr<sup>3+</sup> ion. In contrast, all previous works reported noninteger values of the magnetic moment ( $2.7\text{--}2.9 \mu_B/\text{Cr}^{3+}$ ) [1,2,39]. The observation of integer values of magnetic moment per unit cell satisfies a necessary condition and is an important indicator for the material being a half-metal [17]. This is consistent with the results of the first principles calculations [4,16].

As illustrated in the band diagram in Fig. 1(a), the measured magnetization corresponds to the fully occupied spin-up *t*<sub>2g</sub> orbital of Cr. At low temperatures, Hall resistivity  $\rho_{xy}$  has a linear dependence on the magnetic field, except at very low fields, where magnetization is not saturated and the small curvature is caused by the anomalous Hall effect [Fig. 1(c)]. The linearity in the normal Hall resistance for a wide range of magnetic fields enabled us to extract an electron density of about  $2 \times 10^{18} \text{ cm}^{-3}$  at  $T < 70$  K. The *n*-type samples used for the Andreev reflection measurements to be presented below were taken from the same batch, and the Hall effect measurements consistently yielded carrier densities on the same order of magnitude and electron mobilities of the order of  $10^2 \text{ cm}^2/\text{V s}$  at  $T = 2$  K.

In addition to the ideal magnetization value, the high quality of our *n*-HgCr<sub>2</sub>Se<sub>4</sub> samples is also shown by the strong temperature dependence of the longitudinal resistivity  $\rho_{xx}$ . As depicted in Fig. 1(d),  $\rho_{xx}$  increases by more than 8 orders of magnitude as  $T$  is increased from 10 K to temperatures above the Curie temperature. This is in contrast to the only up to 3 to 4 orders of magnitude change in  $\rho_{xx}$  obtained in previous works [40,41]. The temperature dependence of  $\rho_{xx}$  can be attributed to a metal-insulator transition driven by the ferromagnet-paramagnet transition. In the paramagnetic phase, the chemical potential is located inside the bulk band gap. Below  $T_C$ , the *s*-*d* exchange interaction spin splits the conduction band and gradually raises the chemical potential above the conduction band minimum. The  $\rho_{xx}$  data shown in Fig. 1(d) span from  $\sim 10^{-2} \Omega\text{ cm}$  (metallic) to  $\sim 10^6 \Omega\text{ cm}$  (very insulating). Such a drastic variation in resistivity is comparable to the best values of magnetic semiconductors or other materials exhibiting the colossal magnetoresistance effect [31]. The data in Fig. 1(d) also indicate that the HgCr<sub>2</sub>Se<sub>4</sub> sample has very large magnetoresistance (MR) around the phase transition region. The MR, defined here as  $\text{MR} = \rho_{xx}(0)/\rho_{xx}(B) - 1$ , reaches  $7 \times 10^4$  at  $B = 8$  T and  $T = 110$  K.

We used the Andreev reflection spectroscopy to directly probe the electron spin polarization in HgCr<sub>2</sub>Se<sub>4</sub> [42–44]. It has been used to measure the spin polarization in many ferromagnetic materials [45], including several candidates for half-metals, such as (La,Sr)MnO<sub>3</sub> [46], CrO<sub>2</sub> [26,27], (Ga,Mn)As [29], and EuS [47]. This method is based on the fact that the Andreev reflection probability at the interface between a superconductor and a ferromagnet is partially or completely suppressed by a spin-imbalanced density of states at the Fermi level in the ferromagnet. The spin polarization can be extracted by fitting the conductance spectra to the modified Blonder-Tinkham-Klapwijk (BTK) theory [42–44]. The measurement can be implemented either with point contact geometry [46] or with planar junction geometry [27]. Both geometries have been proven effective in revealing the half-metallicity in CrO<sub>2</sub>, a classic

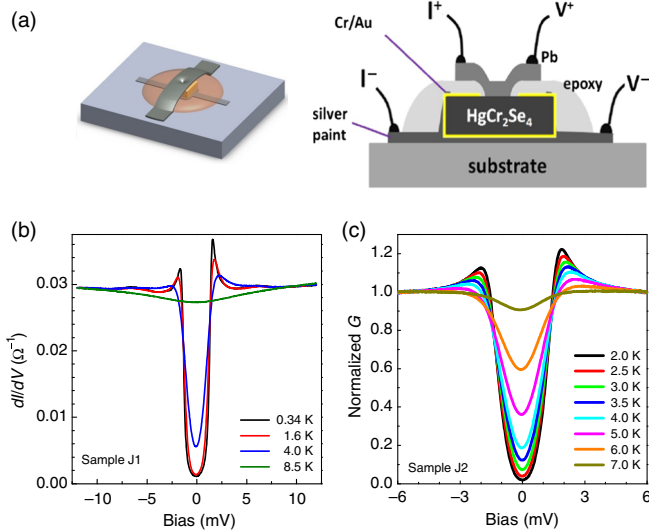


FIG. 2 (color online). (a) Sketch of the  $\text{HgCr}_2\text{Se}_4/\text{Pb}$  planar junctions used for Andreev reflection spectroscopy. (b) Differential conductance  $G(V) = dI/dV$  of the sample J1 plotted as a function of dc bias. (c) Normalized differential conductance  $G(V)/G_N(V)$  spectra for sample J2. Here, the bias  $V$  is defined as the dc voltage of the Pb electrode relative to the Cr/Au electrode at the bottom of the  $\text{HgCr}_2\text{Se}_4$  crystal, and  $G_N(V)$  is normal state differential conductance recorded with a small field ( $\mu_0 H = 0.2$  T) applied.

half-metal that has also been confirmed with other methods, such as the Meservey-Tedrow experiment [27].

Figure 2(a) shows a sketch of the  $\text{HgCr}_2\text{Se}_4/\text{Pb}$  planar junctions used in this Letter. A typical device was fabricated on a lustrous, triangle-shaped surface of a  $\text{HgCr}_2\text{Se}_4$  single crystal [Fig. 1(b), inset]. The differential conductance, defined as  $G(V) = dI(V)/dV$ , was measured as a function of the dc bias voltage  $V$  for  $\text{HgCr}_2\text{Se}_4/\text{Pb}$  junctions using phase-sensitive lock-in detection. The amplitude of the ac modulation was kept sufficiently small in order to avoid heating and other spurious effects. Figure 2(b) shows the conductance curves of sample J1 for temperatures from 0.34 to 8.5 K. The Pb films used in this Letter have a superconducting transition temperature  $T_c = 7.2$  K, nearly identical to the bulk  $T_c$  value in literature. The conductance data at 8.5 K are close to the normal state values,  $G_N(V)$ , which were recorded when a perpendicular magnetic field  $\mu_0 H = 0.2$  T was applied at corresponding temperatures. For sample J1,  $G_N$  is about  $34 \Omega$ , and it has a weak bias dependence.

Many other samples with junction resistances,  $R_N$ , in the range of 14–75  $\Omega$  have also been studied. Although these values are low in comparison to the  $R_N$  of Andreev junctions on other low carrier density materials, an estimate of the junction area based on the point contact models [35] and these junction resistances yields values significantly smaller than the geometric junction areas. Possible explanations for this discrepancy are discussed in detail in the

Supplemental Material [34]. Figure 2(c) shows a set of normalized conductance [ $G(V)/G_N(V)$ ] curves for a  $\text{HgCr}_2\text{Se}_4/\text{Pb}$  junction (sample J2) with  $R_N \approx 14 \Omega$ . The low junction resistance indicates a relatively weak barrier strength at the  $\text{HgCr}_2\text{Se}_4/\text{Pb}$  interface, thus offering the possibility of extraction of the electron spin polarization with the modified BTK theory. This is evidenced by the analysis of the conductance spectra later. These junction resistances are in contrast to those of the planar Andreev junctions of EuS, a magnetic semiconductor with much higher electron densities. In the latter,  $R_N$  is on the order of 10 k $\Omega$  and the  $I$ - $V$  trace is highly nonlinear due to the formation of a Schottky barrier [48]. As shown in Ref. [49], very strong barrier strength could lead to the conductance spectra being hardly discernible from the tunneling spectra between an unpolarized metal and a superconductor. The conductance spectra of our low- $R_N$   $\text{HgCr}_2\text{Se}_4/\text{Pb}$  junctions have the following common characteristics. (1) The subgap conductance is significantly suppressed, as expected for a half-metal. (2) There exist a pair of small, but noticeable, superconducting coherence peaks at the superconducting gap edges, i.e.,  $eV = \pm\Delta$ . The energy gap  $\Delta$  is 1.4–1.5 meV, close to the bulk value of Pb. (3) The heights of both coherence peaks are significantly lower than what is expected of a tunnel junction, and the peak height at the positive bias (see Fig. 2) is greater than that at the negative bias. Such an asymmetry has not been observed in the Andreev reflection spectra of several strongly correlated electron systems, such as heavy fermion superconductor  $\text{CeCoIn}_5$  [50] and ferromagnetic semimetal  $\text{EuB}_6$  [51]. Further work is needed to confirm whether there is a link between the asymmetry and the electron correlation.

The differential conductance data were analyzed with the modified BTK theory [43], in which there are four fitting parameters: spin polarization  $P$ , barrier strength parameter  $Z$ , superconducting gap  $\Delta$ , and inelastic broadening parameter  $\Gamma$ . For the data in this work, we argue that  $\Gamma$  can be approximated to be zero, for the following considerations. (1) In the spectra shown in Fig. 2(b), both a superconducting gap of bulk Pb value and the Pb phonon features (around  $\pm 7$  meV) are apparent, implying a clean  $\text{HgCr}_2\text{Se}_4/\text{Pb}$  interface with minimal lifetime effects. (2) The inelastic broadening energies extracted from Pb/I/Al, and especially from Pb/I/CrO<sub>2</sub> junctions subjected to a similar surface treatment process [27], is on the order of tens of  $\mu\text{eV}$ , 2 orders magnitude smaller than the gap energy. (3) Importantly, we have systematically examined the effects of varying  $\Gamma$ 's on the BTK fits to our data: Best fits with increasing  $\Gamma$ 's up to 0.5 meV result in little change in the extracted  $P$ ; although a larger  $\Gamma$  leads to a decreased  $P$ , it is accompanied by deterioration of the fitting quality, especially near the coherence peaks.

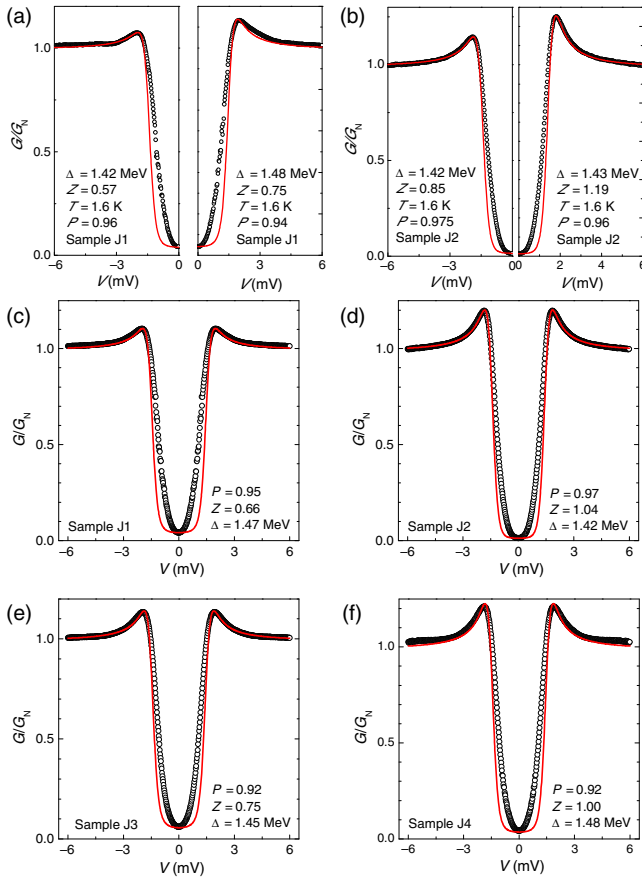


FIG. 3 (color online). Normalized conductance spectra (symbols) before symmetrization [(a),(b), for samples *J1* and *J2*] and after symmetrization [(c)–(f), for samples *J1*–*J4*]. Their fits to the modified BTK theory are shown by lines. The measurement temperature was 1.6 K for all panels.

Figures 3(a) and 3(b) show the normalized conductance curves and the BTK fits with three adjustable parameters (i.e.,  $P$ ,  $Z$ , and  $\Delta$ ) for samples *J1* and *J2*, respectively. The fits were carried out separately for the positive and negative halves of the conductance spectra, namely,  $G(V)$  at  $V > 0$  or  $V < 0$ , and for each sample the extracted  $P$  only differs up to a few percent for different polarities. This justifies the BTK fits with the symmetrized spectra [i.e.,  $G(V) \rightarrow [G(V) + G(-V)]/2$ ] depicted in Figs. 3(c)–3(f) for four junctions. The fits yield  $P = 95\%$ ,  $97\%$ ,  $92\%$ , and  $92\%$ , and  $Z = 0.66$ ,  $1.04$ ,  $0.75$ , and  $1.00$ , for samples *J1*–*J4*, respectively. There is no apparent trend of decreasing  $P$  with increasing  $Z$ , consistent with the previous work on planar  $\text{CrO}_2/\text{Pb}$  junctions [27].

The conductance spectra of the  $\text{HgCr}_2\text{Se}_4/\text{Pb}$  junctions and the extracted high degree of spin polarization from the modified BTK fits have some resemblance to those of  $\text{CrO}_2$  planar junctions, in which spin polarizations of 90% to 97% were obtained for a wide range of barrier strengths ( $Z = 0$  to 2.7) [49]. Nevertheless, it should be pointed out that a 100% spin polarization (or, correspondingly, completely suppressed subgap conductance) has *never* been observed

in any Andreev reflection experiment on  $\text{CrO}_2$  or other half-metals, despite an enormous amount of experimental efforts. Recent theoretical advances have rendered several mechanisms that can account for the small deviation from full spin polarization [52]. These include various spin active scatterings at the superconductor–half-metal interface [25,53–57], the spin-orbit coupling in the superconductor [23] and inelastic scatterings of quasiparticles in the half-metal [58]. These scatterings can relax the rule of spin conservation and can lead to finite conductance at zero bias. Furthermore, the lifting of the particle-hole symmetry away from zero bias brings a conductance correction of the form  $\delta G \propto V^2$ , if  $V$  is not too large [53,56]. Following these models, one would expect a *quadratic* dependence of the junction conductance on the bias voltage. Indeed, this is borne out in the conductance spectra of  $\text{HgCr}_2\text{Se}_4/\text{Pb}$  junctions (Fig. 3): As shown clearly in Fig. 4(a), the low bias  $G(V)$  of sample *J2* deviates substantially from the BTK fit, but it follows a quadratic function very well.

Further evidence for the deviation from conventional BTK-type Andreev reflection comes from the temperature dependence of zero-bias conductance  $G_0$ . As shown in Fig. 4(b),  $G_0$  of sample *J2* roughly follows a  $T^3$  dependence:  $G_0/G_{0,N} \approx (T/T_C)^3$ . In contrast, the modified BTK model predicts substantially smaller  $G_0$  values at intermediate temperatures. The excess of conductance at finite temperatures is qualitatively in good agreement with the calculation of Löfwander *et al.*, with a model of spin active scatterings at a clean superconductor–half-metal interface for the case of singlet-triplet mixing angle  $\vartheta = \pi/4$  [52]. An interesting outcome of their work is that  $G(V)$  vanishes

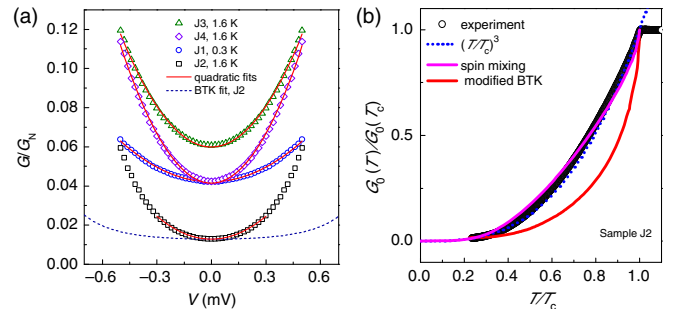


FIG. 4 (color online). (a) Normalized conductances at small bias voltages of  $\text{HgCr}_2\text{Se}_4/\text{Pb}$  junctions at low temperatures ( $T = 0.3$  K for sample *J1* and 1.6 K for samples *J2*–*J4*; symbols). Each of them can be fitted to a quadratic function, i.e.,  $G(V) \sim G_0 + bV^2$  (solid lines). The fit of the conductance spectra of sample *J2* to the modified BTK theory (dotted line) is also shown for comparison. (b) Temperature dependence of the zero-bias conductance  $G_0$  (symbols), which roughly follows a cubic dependence on  $T$  (dotted line). It is also close to the calculations of the spin active scattering model with spin singlet-triplet mixing angle  $\vartheta = \pi/4$  (solid line) [52]. The values derived from the modified BTK fit (solid line at the bottom) deviate strongly from the experimental curve. The data were taken from sample *J2* in zero magnetic field.

at the  $T = 0$  limit. As shown in Figs. 2(b) and 2(c), the zero-bias conductance  $G_0(T)$  saturates at very small values as  $T$  approaches zero. The low temperature  $G_0$  appears to vary from sample to sample [Fig. 4(a)], suggesting the interface quality is important. This may lend support to the disorder assisted spin active scatterings proposed in Ref. [57] for a finite  $G_0$  at  $T = 0$ . The additional conductance induced by the spin active scatterings may be responsible for the underestimation of the spin polarizations in half-metals with the fits to the modified BTK theory reported in the literature [46,52]. The values obtained from the modified BTK fits may only provide lower bounds for the spin polarization.

In summary, the high degree of spin polarization derived from fits to the modified BTK theory, as well as the integer moment magnetization, provides strong evidence for half-metallicity in  $n$ -HgCr<sub>2</sub>Se<sub>4</sub>. This is consistent with the first principles calculations that predicted the half-metallic and Chern semimetallic phases for the  $n$ -doped and undoped HgCr<sub>2</sub>Se<sub>4</sub>, respectively [4]. Furthermore, the small but finite zero-bias conductance and its temperature dependence are compatible with recent theoretical models developed for spin active scatterings, which have been proposed as a venue for realizing the exotic triplet pairing with the superconducting proximity effects in half-metals [22,23,25,53].

This work was supported by the National Basic Research Program of China (Projects No. 2015CB921102, No. 2012CB921703, No. 2011CBA00108, No. 2013CB921700, and No. 2011CBA00110), the National Science Foundation of China (Projects No. 91121003, No. 11374337, and No. 61425035), and the Chinese Academy of Sciences. P.X. acknowledges support from NSF Grant No. DMR-1308613.

---

\*ygshi@iphy.ac.cn

†cong\_ren@iphy.ac.cn

‡yqli@iphy.ac.cn

- [1] P. K. Baltzer, H. W. Lehmann, and M. Robbins, *Phys. Rev. Lett.* **15**, 493 (1965).
- [2] P. K. Baltzer, P. J. Wojtowicz, M. Robbins, and E. Lopatin, *Phys. Rev.* **151**, 367 (1966).
- [3] L. Goldstein, P. Gibart, and A. Selmi, *J. Appl. Phys.* **49**, 1474 (1978).
- [4] G. Xu, H. Weng, Z. Wang, X. Dai, and Z. Fang, *Phys. Rev. Lett.* **107**, 186806 (2011).
- [5] X. G. Wan, A. M. Turner, A. Vishwanath, and S. Y. Savrasov, *Phys. Rev. B* **83**, 205101 (2011).
- [6] P. Hosur and X.-L. Qi, *C. R. Phys.* **14**, 857 (2013) and references therein.
- [7] H. M. Weng, C. Fang, Z. Fang, B. A. Bernevig, and X. Dai, *Phys. Rev. X* **5**, 011029 (2015).
- [8] Z. K. Liu *et al.*, *Science* **343**, 864 (2014).
- [9] Z. K. Liu *et al.*, *Nat. Mater.* **13**, 677 (2014).
- [10] S.-Y. Xu *et al.*, *Science* **349**, 613 (2015).
- [11] B. Q. Lv *et al.*, *Phys. Rev. X* **5**, 031013 (2015).
- [12] X. C. Huang *et al.*, [arXiv:1503.01304](https://arxiv.org/abs/1503.01304).
- [13] R. Yu, W. Zhang, H. J. Zhang, S. C. Zhang, X. Dai, and Z. Fang, *Science* **329**, 61 (2010).
- [14] C. Z. Chang *et al.*, *Science* **340**, 167 (2013).
- [15] H. W. Lehmann, *Phys. Rev.* **163**, 488 (1967).
- [16] S.-D. Guo and B.-G. Liu, *J. Phys. Condens. Matter* **24**, 045502 (2012).
- [17] J. M. D. Coey and S. Sanvito, *J. Phys. D* **37**, 988 (2004).
- [18] M. I. Katsnelson, V. Yu. Irkhin, L. Chioncel, A. I. Lichtenstein, and R. A. de Groot, *Rev. Mod. Phys.* **80**, 315 (2008).
- [19] Materials (e.g., doped manganites) with finite density of states at the Fermi level for both spin orientations are sometimes not considered to be *true* half-metals, since the minority spins also carry magnetic moments that result in noninteger moment magnetization.
- [20] M. Bowen, M. Bibes, A. Barthelemy, J.-P. Contour, A. Anane, Y. Lematre, and A. Fert, *Appl. Phys. Lett.* **82**, 233 (2003).
- [21] G. Schmidt, D. Ferrand, L. W. Molenkamp, A. T. Filip, and B. J. van Wees, *Phys. Rev. B* **62**, R4790 (2000).
- [22] S. B. Chung, H.-J. Zhang, X.-L. Qi, and S.-C. Zhang, *Phys. Rev. B* **84**, 060510(R) (2011).
- [23] M. Duckheim and P. W. Brouwer, *Phys. Rev. B* **83**, 054513 (2011).
- [24] R. S. Keizer, S. T. B. Goennenwein, T. M. Klapwijk, G. Miao, G. Xiao, and A. Gupta, *Nature (London)* **439**, 825 (2006).
- [25] M. Eschrig and T. Lofwander, *Nat. Phys.* **4**, 138 (2008).
- [26] Y. Ji, G. J. Strijkers, F. Y. Yang, C. L. Chien, J. M. Byers, A. Anguelouch, G. Xiao, and A. Gupta, *Phys. Rev. Lett.* **86**, 5585 (2001).
- [27] J. S. Parker, S. M. Watts, P. G. Ivanov, and P. Xiong, *Phys. Rev. Lett.* **88**, 196601 (2002).
- [28] P. G. Steeneken, L. H. Tjeng, I. Elfimov, G. A. Sawatzky, G. Ghiringhelli, N. B. Brookes, and D.-J. Huang, *Phys. Rev. Lett.* **88**, 047201 (2002).
- [29] J. G. Braden, J. S. Parker, P. Xiong, S. H. Chun, and N. Samarth, *Phys. Rev. Lett.* **91**, 056602 (2003).
- [30] M. A. Korotin, V. I. Anisimov, D. I. Khomskii, and G. A. Sawatzky, *Phys. Rev. Lett.* **80**, 4305 (1998).
- [31] J. M. D. Coey, M. Viret, and S. von Molnar, *Adv. Phys.* **48**, 167 (1999).
- [32] R. Schiller and W. Nolting, *Solid State Commun.* **118**, 173 (2001).
- [33] T. Dietl and H. Ohno, *Rev. Mod. Phys.* **86**, 187 (2014).
- [34] See Supplemental Material at <http://link.aps.org/supplemental/10.1103/PhysRevLett.115.087002>, which includes Refs. [35–38], for details on sample preparation, additional data, and discussions of the junction resistance.
- [35] Y. G. Naidyuky and I. K. Yanson, *J. Phys. Condens. Matter* **10**, 8905 (1998).
- [36] D. Daghero and R. S. Gonnelli, *Supercond. Sci. Technol.* **23**, 043001 (2010).
- [37] B. J. van Wees, P. de Vries, P. Magnee, and T. M. Klapwijk, *Phys. Rev. Lett.* **69**, 510 (1992).
- [38] P. Xiong, G. Xiao, and R. B. Laibowitz, *Phys. Rev. Lett.* **71**, 1907 (1993).

- [39] M. I. Auslender, A. A. Samokhvalov, N. I. Solin, and I. Yu. Shumilov, *Sov. Phys. JETP* **67**, 2516 (1988).
- [40] A. A. Samokhvalov, D. A. Gizhevskii, N. N. Loshkareva, T. I. Arbuzova, M. I. Simonova, and N. M. Chebotayev, *Sov. Phys. Solid State* **23**, 2016 (1981).
- [41] N. I. Solin, V. V. Ustinov, and S. V. Naumov, *Phys. Solid State*, **50**, 901 (2008).
- [42] G. E. Blonder, M. Tinkham, and T. M. Klapwijk, *Phys. Rev. B* **25**, 4515 (1982).
- [43] I. I. Mazin, A. A. Golubov, and B. Nadgorny, *J. Appl. Phys.* **89**, 7576 (2001).
- [44] G. T. Woods, R. J. Soulen, I. Mazin, B. Nadgorny, M. S. Osofsky, J. Sanders, H. Srikanth, W. F. Egelhoff, and R. Datla, *Phys. Rev. B* **70**, 054416 (2004).
- [45] S. K. Upadhyay, A. Palanisami, R. N. Louie, and R. A. Buhrman, *Phys. Rev. Lett.* **81**, 3247 (1998).
- [46] R. J. Soulen, Jr., J. M. Byers, M. S. Osofsky, B. Nadgorny *et al.*, *Science* **282**, 85 (1998).
- [47] C. Ren, J. Trbovic, R. L. Kallaher, J. G. Braden, J. S. Parker, S. von Molnár, and P. Xiong, *Phys. Rev. B* **75**, 205208 (2007).
- [48] C. Ren, J. Trbovic, P. Xiong, and S. von Molnár, *Appl. Phys. Lett.* **86**, 012501 (2005).
- [49] J. S. Parker, Ph.D thesis, Florida State University, 2003.
- [50] W. K. Park, J. L. Sarrao, J. D. Thompson, and L. H. Greene, *Phys. Rev. Lett.* **100**, 177001 (2008).
- [51] X. H. Zhang, S. von Molnár, Z. Fisk, and P. Xiong, *Phys. Rev. Lett.* **100**, 167001 (2008).
- [52] T. Löfwander, R. Grein, and M. Eschrig, *Phys. Rev. Lett.* **105**, 207001 (2010) and references therein.
- [53] B. Béri, J. N. Kupferschmidt, C. W. J. Beenakker, and P. W. Brouwer, *Phys. Rev. B* **79**, 024517 (2009).
- [54] J. N. Kupferschmidt and P. W. Brouwer, *Phys. Rev. B* **80**, 214537 (2009).
- [55] J. Linder, M. Cuoco, and A. Sudbø, *Phys. Rev. B* **81**, 174526 (2010).
- [56] J. N. Kupferschmidt and P. W. Brouwer, *Phys. Rev. B* **83**, 014512 (2011).
- [57] F. B. Wilken and P. W. Brouwer, *Phys. Rev. B* **85**, 134531 (2012).
- [58] B. Béri, *Phys. Rev. B* **79**, 245315 (2009).